

## Elastic deformation and stability in pentagonal nanorods with multiple twin boundaries

This article has been downloaded from IOPscience. Please scroll down to see the full text article.

2002 J. Phys.: Condens. Matter 14 113

(<http://iopscience.iop.org/0953-8984/14/1/310>)

View [the table of contents for this issue](#), or go to the [journal homepage](#) for more

Download details:

IP Address: 171.66.16.238

The article was downloaded on 17/05/2010 at 04:43

Please note that [terms and conditions apply](#).

# Elastic deformation and stability in pentagonal nanorods with multiple twin boundaries

Feng Ding<sup>1,2</sup>, Hui Li<sup>1</sup>, Jinlan Wang<sup>1</sup>, Weifeng Shen<sup>1</sup> and Guanghou Wang<sup>1,3</sup>

<sup>1</sup> National Laboratory of Solid State Microstructures and Department of Physics, Nanjing University, Nanjing 210093, People's Republic of China

<sup>2</sup> Department of Physics, Qufu Normal University, Qufu 273165, People's Republic of China

E-mail: ghwang@nju.edu.cn

Received 6 July 2001, in final form 25 October 2001

Published 7 December 2001

Online at [stacks.iop.org/JPhysCM/14/113](http://stacks.iop.org/JPhysCM/14/113)

## Abstract

In this paper we calculate and discuss the elastic deformation in a new kind of nanorod, a pentagonal rod with multiple twin boundaries, on the basis of elastic theory. Present theory shows that the central part of the pentagonal rod is highly compressed whereas the outer part is tensioned. The average bond length in the central part is about 1–2% shorter than that in the outer part. Present theory also indicates that the nanorod structure is metastable and will disappear at a certain critical size (around several tens of nanometres).

## 1. Introduction

Recently, nanometre-sized particles and rods have become a focus of interest due to their remarkable mechanical properties, as well as their electronic, optical and magnetic properties, which are often different from those of the corresponding bulk material [1–4]. The structure of nanometre-sized particles and rods is the basis for the study of their physical and chemical properties. Multiply twinned particles (MTPs) (including icosahedra, decahedra and Marks decahedra) with five-fold symmetry axes are a type of structure unique to nanometre-sized particles [5–7]. The structure and the stability of these MTPs have been well documented [8].

For nanorods, the structure with multiple twin boundaries is hardly ever observed. Small metal rods with a size of less than several nanometres often have a shell-like or helical structure [9, 10], whereas large rods often have the same structure as the corresponding bulk material [11].

Recently, a new kind of nanorod—a pentagonal copper nanorod with five-fold symmetry—has been fabricated by Lisiecki *et al* [12, 13]. These rods are of the order of 1  $\mu\text{m}$  long and have a diameter up to 25 nm. The five-fold symmetry is very interesting since it means that

<sup>3</sup> To whom the correspondence should be addressed.

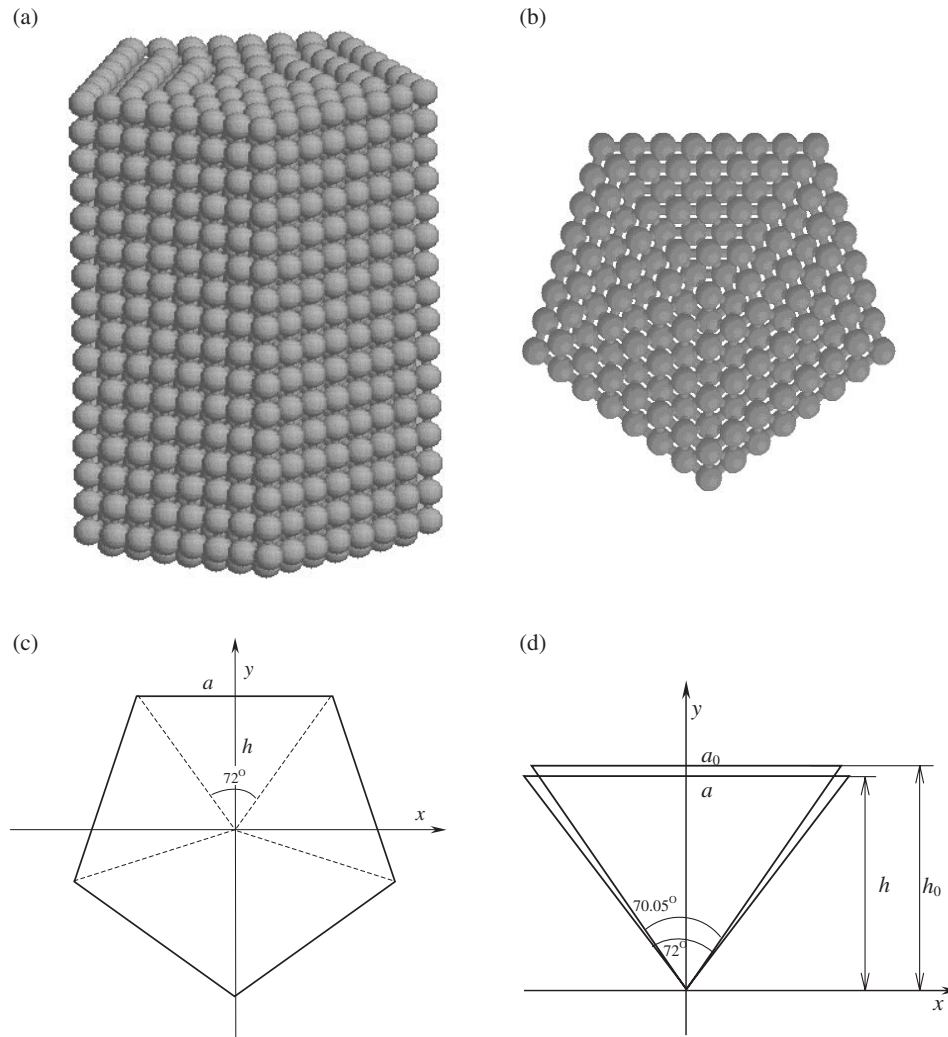


**Figure 1.** The structure of pentagonal nanorods with MTRs. (a) A three-dimensional graph of an MTR. (b) The projection of the nanorod from the axial direction ( $z$  direction). (c) An MTR can be divided into five triangular rods connected to each other by (111) twin boundaries. The broken lines indicate the twin boundaries. (d). Each triangular rod with edge lengths  $a$  and  $h$  is deformed by a free triangular rod with fcc structure and edge lengths  $a_0$  and  $h_0$ .

the structure of these rods is different from that of the corresponding bulk material (Cu bulk material has an fcc structure). This structure has been explained in terms of well-truncated decahedra [12].

As figure 1 shows, such a pentagonal nanorod contains five triangular rods. As in their bulk material structure, these triangular rods have an fcc structure and are connected to each other by (111) twin boundaries (the broken lines in figure 1(c) indicate twin boundaries). Thus, we can call it a multiply twinned rod (MTR). It is well known that the subunits in MTPs are deformed; the 20 tetrahedra in an icosahedron and the five tetrahedra in a decahedron are deformed because of the geometrical configuration of the icosahedron and decahedron [8]. In a similar way the five triangular rods in the pentagonal rod are also deformed.

Figure 1(c) shows the structure of a five-fold nanorod and figure 1(d) shows a triangular rod. The angle between two adjacent twin boundaries is  $72^\circ$  whereas the angle between the two (111) facets of an undeformed fcc structure is  $70.525^\circ$ . In order to form a pentagonal rod without any gaps these triangular rods must be deformed, and so elastic deformation and elastic energy exist in the MTR. It is the elastic energy that contributes to the instability of the five-fold structure, and such a structure will disappear at large enough size. The elastic deformation and the elastic energy in the MTRs are of fundamental importance for studying the stability and the properties of the MTRs.

The elastic deformation in MTRs was first studied by Ino with the assumption of uniform deformation [8]. However, we found that this assumption is not reasonable [14]. As for Ni and Lennard-Jones icosahedral clusters, the numerical simulation results show that the bond length increases on moving from the centre to the surface [6, 15]. In this paper, we will discuss elastic deformation and stability in MTRs.

## 2. Calculation of the distribution of elastic deformation in MTRs

Apparently each triangular subunit in the pentagonal rod has the same elastic deformation for reasons of symmetry. So we can consider just one triangular rod in the MTR (as shown in figure 1(d)) instead of five. We assume that the nanorods have the same elastic modulus as the corresponding bulk material because each triangular rod has same the structure as the corresponding bulk material (here only those materials with an fcc structure are considered because Cu has an fcc structure). The matrix of elastic stiffness constants in this coordinate system is [8]:

$$\begin{pmatrix} C'_{11} & C_{12} & C'_{13} & 0 & 0 & 0 \\ C_{12} & C_{11} & C_{12} & 0 & 0 & 0 \\ C'_{13} & C_{12} & C'_{11} & 0 & 0 & 0 \\ 0 & 0 & 0 & C_{44} & 0 & 0 \\ 0 & 0 & 0 & 0 & C'_{44} & 0 \\ 0 & 0 & 0 & 0 & 0 & C_{44} \end{pmatrix} \quad (1)$$

where  $C'_{11} = \frac{1}{2}(C_{11} + C_{12} + 2C_{44})$ ,  $C'_{13} = \frac{1}{2}(C_{11} + C_{12} - 2C_{44})$ ,  $C'_{44} = \frac{1}{2}(C_{11} - C_{12})$  and  $C_{ij}$  is the elastic modulus of the corresponding fcc bulk material. We assume that the triangular rod was deformed by a free triangular rod with an fcc structure (figure 1(d)). We would first like to make some suggestions for simplifying the problem:

- (1) As in icosahedral clusters [14], the MTR has a shell-like structure. So we can assume that the difference in the elastic deformation at different places in same layer is very small. This means that the elastic deformation and the elastic stress depend on coordinate  $y$  only.
- (2) In each of the three surfaces of the triangular rod, the shear deformation components parallel to the surface are zero due to the symmetry of its twin boundaries and the boundary condition at the external surface. Thus it is reasonable to neglect the shear components of the elastic deformation and the elastic stress in the triangular rod.

We denote by  $e_{xx}(y)$ ,  $e_{yy}(y)$ ,  $e_{zz}$  and  $\sigma_{xx}(y)$ ,  $\sigma_{yy}(y)$ ,  $\sigma_{zz}(y)$  the elastic deformation and elastic stress components along the  $x$ ,  $y$  and  $z$  directions, where the  $z$  direction is the axial direction of the MTR.

As shown in figure 1(d), the edge length on the surface is deformed from  $a_0$  to  $a = (1 + e_{xx}(y))a_0$  and the triangular height is deformed from  $h_0$  to  $h = (1 + \frac{1}{h} \int_0^h e_{yy}(\xi) d\xi)h_0$ . In order to form an MTR without any gap, the ratio of  $a$  to  $h$  should be  $a/h = 2 \tan(\pi/5) = 1.4531$ . In fact, this relationship should hold for any small subunit from the centre to  $y$  because the

small subunit from the centre to  $y$  is deformed by a small free triangular rod with fcc structure. Thus, we have a constrained equation:

$$\frac{1 + e_{xx}(y)}{1 + \frac{1}{y} \int_0^y e_{yy}(\xi) d\xi} = 1 + \delta \quad y \in [0, h] \quad (2)$$

where  $\delta = 0.027066$ . Because both  $e_{xx}(y)$  and  $e_{yy}(y)$  are much smaller than 1.0, the above equation can be simplified as

$$e_{xx}(y) - \frac{1}{y} \int_0^y e_{yy}(\xi) d\xi = \delta. \quad (3)$$

By denoting the external pressure under which the MTR grows as  $P_0$ , we have a boundary condition:

$$\sigma_{yy}(h) = -P_0. \quad (4)$$

(3) Supposing that the pressure perpendicular to the twin boundaries is  $\sigma_{xx}(y)$ . In order to hold the dynamic balance, the total external force on any part of the triangular rod from  $y - y + dy$  is zero. This leads to another equation:

$$\sigma_{xx} = \zeta \frac{d\sigma_{yy}}{d\zeta} + \sigma_{yy} \quad y \in [0, h]. \quad (5)$$

Omitting the influence of the shear components of stress tensor and deformation tensor, Hooke's law can be write as:

$$\begin{pmatrix} \sigma_{xx}(z) \\ \sigma_{yy}(z) \\ \sigma_{zz}(z) \end{pmatrix} = \begin{pmatrix} C'_{11} & C_{12} & C'_{13} \\ C_{12} & C_{11} & C_{12} \\ C'_{13} & C_{12} & C'_{11} \end{pmatrix} \begin{pmatrix} e_{xx}(z) \\ e_{yy}(z) \\ e_{zz}(z) \end{pmatrix}. \quad (6)$$

The reverse of Hooke's law is:

$$\begin{pmatrix} e_{xx} \\ e_{yy} \\ e_{zz} \end{pmatrix} = \begin{pmatrix} A_{11} & A_{12} & A_{13} \\ A_{12} & A_{22} & A_{12} \\ A_{13} & A_{12} & A_{11} \end{pmatrix} \begin{pmatrix} \sigma_{xx} \\ \sigma_{yy} \\ \sigma_{zz} \end{pmatrix} \quad (7)$$

where

$$(A_{ij}) = \frac{1}{\Delta} \begin{pmatrix} C_{11}C'_{11} - C_{12}^2 & C_{12}C'_{13} - C_{12}C'_{11} & C_{12}^2 - C_{11}C'_{13} \\ C_{12}C'_{13} - C_{12}C'_{11} & C_{11}^2 - C_{13}^2 & C_{12}C'_{13} - C_{12}C'_{11} \\ C_{12}^2 - C_{11}C'_{13} & C_{12}C'_{13} - C_{12}C'_{11} & C_{11}C'_{11} - C_{12}^2 \end{pmatrix}$$

and

$$\Delta = C_{11}C_{11}'^2 - 2C_{11}'C_{12}^2 + 2C_{12}^2C_{13}' - C_{11}C_{13}'^2.$$

For an nanorod of infinite length,  $e_{zz}$  should be constant, so we have

$$A_{13}\sigma_{xx} + A_{12}\sigma_{yy} + A_{11}\sigma_{zz} = e_{zz} = \text{const}. \quad (8)$$

Introducing formulae (5), (7) and (8) into equation (3), we can get an Euler differential equation:

$$\zeta^2 \frac{d^2\sigma_{yy}}{d\zeta^2} + 3\zeta \frac{d\sigma_{yy}}{d\zeta} + \beta\sigma_{yy} + \gamma = 0 \quad (9)$$

where

$$\zeta = \frac{y}{h} \quad \beta = \frac{(A_{11}^2 + A_{12}^2 - A_{13}^2 - A_{11}A_{22})}{(A_{11}^2 - A_{13}^2)} \quad \text{and} \quad \gamma = \frac{(A_{13} - A_{12})e_{zz} - A_{11}\delta}{(A_{11}^2 - A_{13}^2)}.$$

This equation can be simply solved as

$$\sigma_{yy} = P_{y1}\zeta^n + P_{y0} \quad (10)$$

where  $n = \sqrt{1-\beta} - 1$ ,  $P_{y1} = (P_0 + \frac{\gamma}{\beta})$ ,  $P_{y0} = -\gamma/\beta$ . From the above equation and equations (5) and (8), we can get the other components of elastic stress:

$$\begin{aligned}\sigma_{xx} &= P_{x1}\zeta^n + P_{x0} \\ \sigma_{zz} &= P_{z1}\zeta^n + P_{z0}\end{aligned}\quad (11)$$

where

$$\begin{aligned}P_{x1} &= (1+n) \left( P_0 + \frac{\gamma}{\beta} \right) & P_{x0} &= -\frac{\gamma}{\beta} & P_{z1} &= -\left( \frac{A_{13}(1+n) + A_{12}}{A_{11}} \right) \left( P_0 + \frac{\gamma}{\beta} \right) \\ P_{z0} &= \frac{(A_{12} + A_{13}) \frac{\gamma}{\beta} + e_{zz}}{A_{11}}.\end{aligned}$$

From Hooke's law, the three components of elastic deformation are

$$\begin{aligned}e_{xx} &= D_{11}\zeta^n + D_{12} \\ e_{yy} &= D_{22}\zeta^n + D_{21} \\ e_{zz} &= \text{const}\end{aligned}\quad (12)$$

where

$$\begin{aligned}D_{11} &= \left( P_0 + \frac{\gamma}{\beta} \right) \left( A_{11}(1+n) + A_{12} - \frac{A_{13}^2(1+n) + A_{12}A_{13}}{A_{11}} \right) \\ D_{12} &= \frac{\gamma}{\beta} \left( \frac{A_{13}^2 + A_{12}A_{13}}{A_{11}} - A_{11} - A_{12} \right) + \frac{A_{13}}{A_{11}} e_{zz} \\ D_{22} &= \left( P_0 + \frac{\gamma}{\beta} \right) \left( A_{12}(1+n) + A_{22} - \frac{A_{13}A_{12}(1+n) + A_{12}^2}{A_{11}} \right) \\ D_{21} &= \frac{\gamma}{\beta} \left( \frac{A_{12}^2 + A_{12}A_{13}}{A_{11}} - A_{22} - A_{12} \right) + \frac{A_{12}}{A_{11}} e_{zz}.\end{aligned}$$

The distribution of elastic energy density and the average elastic energy in the MTR are

$$\begin{aligned}\varepsilon(\zeta) &= E_2\zeta^{2n} + E_1\zeta^n + E_0 \\ \bar{\varepsilon} &= \frac{2}{2+2n} E_2 + \frac{2}{2+n} E_1 + E_0\end{aligned}\quad (13)$$

where

$$\begin{aligned}E_2 &= D_{11}P_{x1} + D_{22}P_{y1} & E_1 &= D_{11}P_{x0} + D_{12}P_{x1} + D_{22}P_{y0} + D_{21}P_{y1} + e_{zz}P_{21} \\ E_0 &= D_{12}P_{x0} + D_{21}P_{y0} + e_{zz}P_{z0}.\end{aligned}$$

### 3. Discussion

#### 3.1. The distribution of elastic deformation in MTRs.

Figures 2(a)–(c) show the distribution of elastic deformation, elastic stress and elastic energy in the MTRs of Ag, Au and Cu at zero surface pressure ( $P_0 = 0$ ) and zero deformation in the axial direction ( $e_{zz} = 0$ ). It is clear that the central part of the MTR is more compressed than the outer part, and the elastic energy in the central part is many times higher than that in outer part. The elastic stress  $\sigma_{xx}$  in the central part (about  $y < 0.4h$ ) is negative whereas  $\sigma_{xx}$  in the outer part (about  $y > 0.4h$ ) is positive. This indicates that the central part of the icosahedron is compressed whereas the outer part is tensioned in the  $x$  direction. Such a distribution of the elastic stress is favourable for keeping the force balanced.

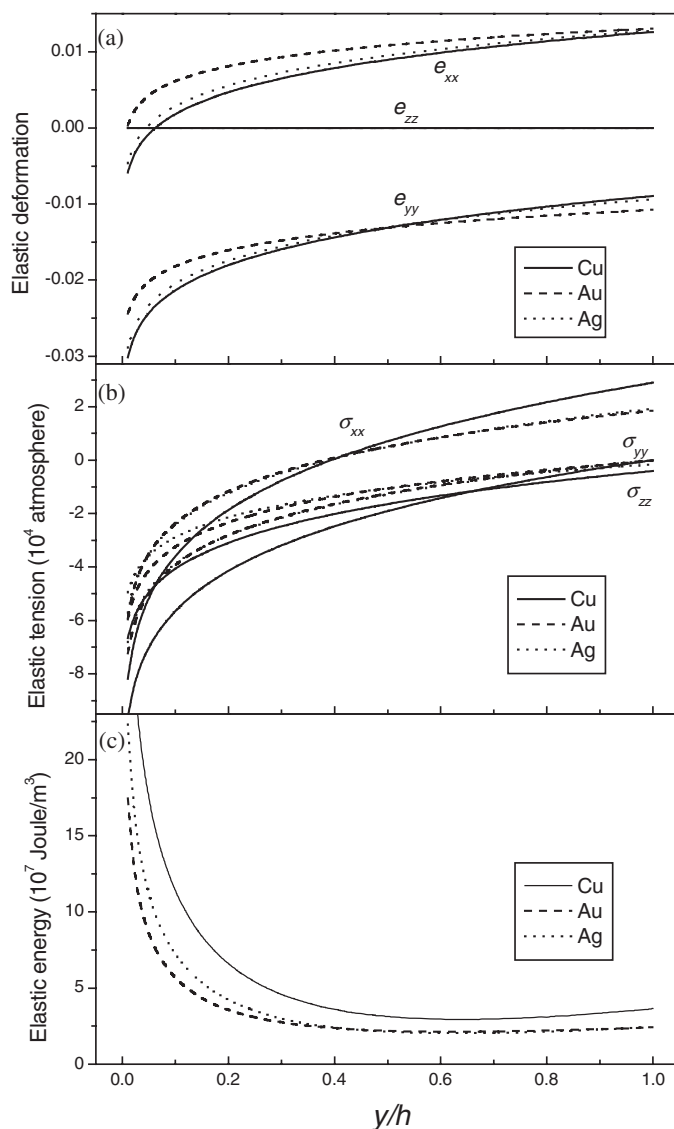


**Figure 2.** The elastic deformation (a), tension (b) and energy distribution (c) in the MTRs of Cu (full curves), Au (broken curves) and Ag (dotted curves) at zero external pressure ( $P_0 = 0$ ) and zero deformation in the axial direction ( $e_{zz} = 0$ ).

From figure 2(b) we can see that the elastic pressure ranges from 50 000 to 80 000 atmospheres in the centre whereas the tension in outer part is about 20 000 atmospheres. It is well known that many physical and chemical properties of materials (such as the Raman spectrum, density of states (DOS) and melting point) depend on the pressure. So a high non-uniform distribution of elastic stress in the MTRs may make these properties different from those of the corresponding bulk material. Further study about how the non-uniform elastic deformation in MTRs influences their properties is needed.

### 3.2. Comparison with the results of numerical simulation

In order to test our theory, the stable structure of Ag, Au and Cu MTRs with 12 shells (containing 456 atoms per layer along the axial direction) were simulated numerically. The interaction between atoms is the widely used TB-SAM (second moment approximation of the tight-binding scheme) potential [16], and the parameters of these materials are same as those in [16]. The numerical simulation begins with a given MTR structure, and the steepest descent method was used to make the given structure reach a local stable state. After we obtained the local stable state, the average bond length deformation in each shell and that between adjacent shells were calculated. The components of elastic deformation along the  $x$  and  $y$  directions were calculated according to the average bond length deformation. The results are shown in figures 3(a)–(c).

Figures 3(a)–(c) show the elastic deformation in Ag, Au and Cu MTRs. The scatter symbols in these figures are the results of the numerical simulation and the full curves are the results of the present theory. From these figures we can conclude that the numerical results prove the validity of the present theory since the numerical and theoretical results are in very good agreement. Both the deformation along the  $x$  direction and that along the  $y$  direction increase on moving from the centre to the surface, which means that the average bond length in the central part is about 1–2% shorter than that in the outer part.

### 3.3. The stability of MTRs

In order to discuss the stability of the MTR structure we must consider other rods with bulk structure (fcc structure). There are many possible shapes for nanorods with an fcc structure. Here we consider hexagonal rods because of their lower surface energy. As shown in figure 4, four of the six surfaces of such a rod are (111) facets and the other two are (100) facets. The surface energies of the (111) facet and the (100) facet of the fcc structure are often lower than those of other kinds of facets.

The difference in energy between an MTR and bulk material with same volume is

$$\Delta E_{\text{MTR}} = 5\gamma_{100}al + \frac{5}{2\cos(\frac{3}{10}\pi)}\gamma_t al + \frac{5}{2}la^2 \sin\left(\frac{3}{10}\pi\right)\bar{\epsilon} \quad (14)$$

where  $l$  is the height of the rod and  $\gamma_{100}$  and  $\gamma_t$  is the surface energy density of (100) facets and the twin boundaries. The first term of equation (14) is the surface energy of the five external surfaces, the second term is the surface energy of the five twin boundaries and the third term is the elastic energy in the MTR. The first two terms are proportional to the edge length  $a$  whereas the third term is proportional to  $a^2$ . The surface energy dominates for thin rods whereas the elastic energy dominates for large ones. The energy difference between a hexagonal rod and the bulk material with same volume is

$$\Delta E_{\text{hex}} = 4\gamma_{111}b_1l + 2\gamma_{100}b_2l \quad (15)$$

where  $\gamma_{111}$  is the surface energy density of (111) facets and  $b_1, b_2$  are the edge lengths of the hexagonal rod (in figure 4(b)). The volume of such a hexagonal rod with unit height is  $V = 1.633b_1b_2 + 0.94281b_1^2$ . For hexagonal rods with constant volume and height, the energy varies with the ratio of  $b_2$  to  $b_1$ . By simple calculation, we can get the ratio of  $b_2$  to  $b_1$  of the hexagonal rod with the lowest energy when its volume and height are kept constant:  $b_2/b_1 = 2(\frac{\gamma_{111}}{\gamma_{100}} - 0.5773)$ . Figure 5 shows the volume dependence of the energy difference between Cu MTRs and hexagonal rods with the lowest energy. It is clear that the energy of such a hexagonal rod is lower than that of an MTR with same volume. This indicates that the MTR structure is a kind of metastable structure but the global minimum structure of the



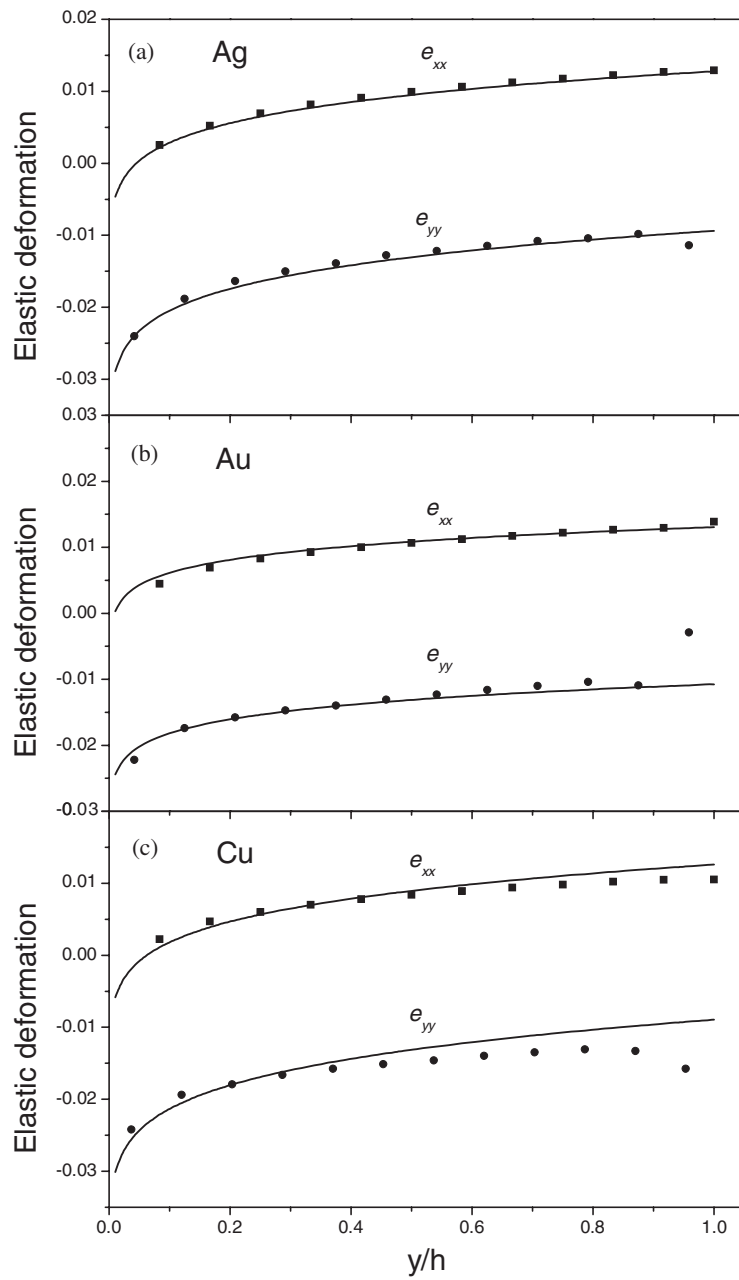


**Figure 3.** Comparison of the results of the numerical simulation (scatter symbols) with those of the present theory (curves) for elastic deformation for Au (a), Ag (b) and Cu (c) at zero external pressure ( $P_0 = 0$ ) and zero deformation in the axial direction ( $e_{zz} = 0$ ).

nanorods. Similar results are obtained for other fcc metals such Au, Ag and Ni. Maybe this is the reason why nanorods with multiple twin structure are rarely observed.

Whereas the MTR structure can exist at nanometre size, it will disappear with an increase in size because of its non-periodic structure. At a certain critical size the MTR structure is

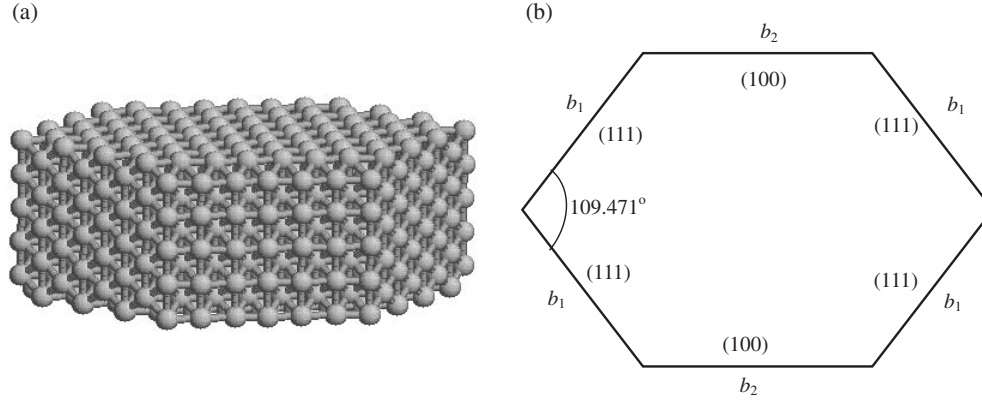


**Figure 4.** The structure of hexagonal rods with an fcc structure. (a) A three-dimensional photo of a section of a hexagonal rod. (b) The structure of a projection of the hexagonal rod with edge lengths  $b_1$  and  $b_2$ , (111) and (100) denoting the two kinds of crystal plane in the fcc structure.

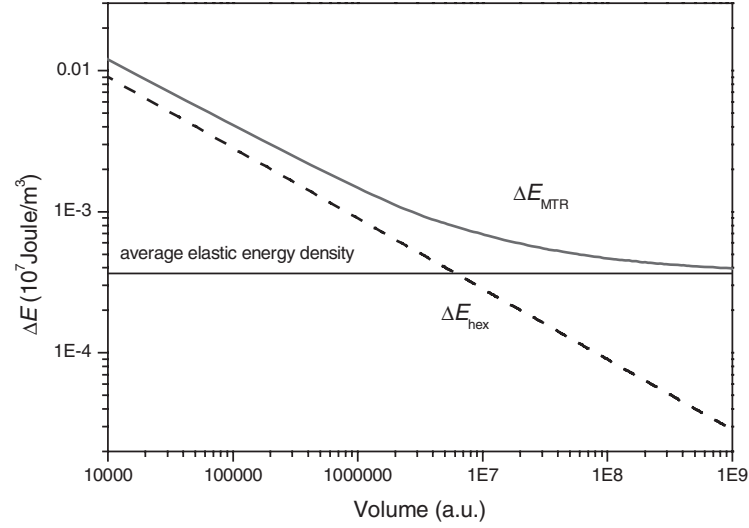


**Figure 5.** The solid curve (broken line) is the volume dependence of the energy difference between the MTRs (hexagonal rods) and the corresponding bulk materials.

impossible to stabilize: in fact it is the elastic energy in an MTR that makes it unstable. If an MTR is unstable, a gap of  $9.75^\circ$  will appear at one of its five twin boundaries (as shown in figure 6) and the elastic energy will disappear. So we can give a criterion for instability of the MTR structure: an MTR will be unstable if the energy of the MTR with a gap of  $9.75^\circ$  is lower than that of a perfect MTR. We can get the critical size  $a_c$  of the MTR from this criterion:

$$a_c = \frac{4\gamma_{111} - 2\gamma_t}{5 \sin(\frac{3}{5}\pi)\bar{\epsilon}}. \quad (16)$$

Table 1 lists the average elastic energy density and the critical size for some metals with an fcc structure. The critical size for these metals varies from 20 to 100 nm. For Cu the critical size is 53.1 nm, which is in good agreement with the size of the rods obtained in experiments (25 nm).

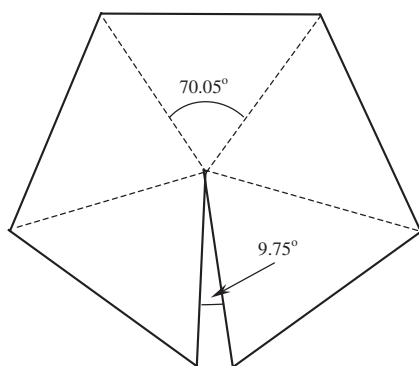


**Figure 6.** A gap of  $9.75^\circ$  will appear at one of the twin boundaries if an MTR becomes unstable with increasing size.

**Table 1.** The average elastic energy density in MTRs of some metals with bulk fcc structure and their critical size.

	Cu	Au	Ag	Pb	Ni	Al	Pd
Elastic energy ( $10^8$ erg $\text{cm}^{-3}$ )	3.646	2.414	2.457	0.7198	12.77	1.648	3.777
Critical size $a$ (nm)	53.1	68.2	51.4	78.8	20.4	86.2	49.6

In summary: the elastic deformation in a new kind of nanorod, pentagonal nanorods with MTRs, was calculated based on elastic theory. The numerical simulation of Au, Ag and Cu MTRs proves the validity of the present theory. The stability and instability of the MTRs was discussed on the basis of the present theory. The MTR structure was found to be a quasistable structure and such a structure will disappear at a size of around several tens of nanometres.

### Acknowledgments

This work performed under the auspices of the National Nature Foundation of China (no 29890210) and the Nature Science Foundation of Shandong China (no Q99A04).

### References

- [1] Alivisatos A P 1996 *Science* **271** 933
- [2] Glossman M D, Iniguez M P and Alfonso J A 1992 *Z. Phys. D* **22** 541
- [3] Lisiecki I and Pileni M P 1993 *J. Am. Chem. Soc.* **115** 3887
- [4] Petit C, Lixon P and Pileni M P 1993 *J. Phys. Chem.* **97** 12 974
- [5] Martin T P 1996 *Phys. Rep.* **273** 199
- [6] Cleveland C L and Landman U 1991 *J. Chem. Phys.* **94** 7376
- [7] Miehle W, Kandler O and Leisner I 1989 *J. Chem. Phys.* **91** 5940
- [8] Ino S 1969 *J. Phys. Soc. Japan* **27** 941
- [9] Bilalbegovic G 2000 *Comput. Mater. Sci.* **18** 333–8
- [10] Tosatti E, Prestipino S, Kostlmeier S, Dal Corso A and Di Tolla F D 2001 *Science* **291** 288–90
- [11] Wang Z L, Mohamed M B, Link S and El-Sayed M A 1999 *Surf. Sci.* **440** 809–14
- [12] Lisiecki I, Filankembo A, Sack-Kongehl H, Weiss K, Pileni M P and Urban J 2000 *Phys. Rev. B* **61** 4968–74
- [13] Lisiecki I *et al* 2000 *Langmuir* **16** 8807–8
- [14] Ding F, Li H, Wang J, Shen W and Wang G 2001 *Int. J. Mod. Phys. B* **15** 1947–57
- [15] Farges J, de Feraudy M F, Raoult B and Torchet G 1988 *Adv. Chem. Phys.* **70** 45
- [16] Cleri F and Rosato V 1993 *Phys. Rev. B* **48** 22